JSEE Vol. 21, No. 4, 2019 DOI:10.48303/jsee.2019.243311

Modification of Park-Ang Damage Index to Accommodate Effect of Aftershocks on RC Structures

Morteza Bastami[1*] and Behrouz Ebrahimi[2]

1. Associate Professor, Structural Engineering Research Center, International Institute of Earthquake Engineering and Seismology (IIEES), Tehran, Iran,
*Corresponding Author; email: m.bastami@iiees.ac.ir
2. M.Sc. Graduate, University of Kurdistan, Sanandaj, Iran

Received: 07/06/2020
Accepted: 11/10/2020

ABSTRACT

Seismic design codes do not consider the effects of aftershocks on structures. Moreover, most damage estimation methods disregard the effects of consecutive earthquakes. Recent earthquakes have demonstrated that the aftershocks can cause major damage to mainshock-damaged structures. After a strong seismic event, it should be determined if a mainshock-damaged building is safe for reoccupation in the event of aftershocks. This study examined the effects of both the main shock and aftershocks on the damage index of reinforced concrete (RC) structures. Records from 19 mainshocks that occurred in the Japan seismic region with moment magnitudes of greater than 4 were examined. More than 100 acceleration time series from these events (mainshock + aftershock events) were applied to evaluate the damage index. Seismic damage analysis was performed on a series of RC columns and RC frames. The natural period of these structures varied from 0.1 to 2.5 s. The damage index introduced by Park and Ang was employed to estimate the structural damage. Acceleration time series were applied to the structures in two steps. First, only mainshocks were applied to the structures and the damage index was obtained. Next, both the mainshock and aftershocks were applied to the structures and structures damaged by a mainshock were analyzed under periodic aftershock events. The results showed that the increase in structural period and the PGA of the aftershocks amplified the damage index under the effects of the aftershocks. A modification to Park-Ang damage index is proposed using a dimensionless term to accommodate the effect of aftershocks.

Keywords:
Aftershock; Damage index; RC structures; Natural period

1. Introduction

Although recent strong earthquakes such as the 1994 Northridge, 1999 Kocaeli, 2010 Haiti, 2012 Ahar-Varzaghan, 2015 Nepal and 2017 Sarpol-e Zahab earthquakes have been followed by many aftershocks, the effects of aftershocks are not considered in seismic design codes. Aftershocks have important emotional and structural consequences. In earthquake-stricken areas in which buildings have been damaged or destroyed, aftershocks increase fear and anxiety in residents and can disrupt relief and rescue operations. Moreover, mainshock-damaged structures that are visually stable could collapse during an aftershock because the stiffness of the structure decreases as an effect of the mainshock, and the structure no longer has its initial resistance to new lateral loading. After the 2011 Tohoku earthquake with a moment magnitude of 9.0, aftershocks in some areas caused more damage than the mainshock.

Investigation of the characteristics of mainshocks

and their aftershocks reveals that there are differences in the ground motion parameters. For example, the predominant periods of aftershocks and mainshocks can be thoroughly dissimilar as the predominant period for the set of mainshocks is longer than that of the aftershocks [1]. This means that the structure could experience a variety of seismic waves with different characteristics that can increase the chance of seismic amplification. Sunasaka and Kiremidjian [2] proposed a method to evaluate damage caused by mainshock-aftershock earthquake sequences. They determined that cumulative damage from mainshock-aftershock sequences could be significantly higher than the damage caused only by the mainshock. Gallagher et al. [3] investigated structures those damaged during aftershocks and found that considerable damage to buildings can occur from aftershocks.

Amadio et al. [4] studied the non-linear response of SDOF systems under repeated ground motion. Their analysis was performed on a moment-resisting steel frame and showed a diminution of the behavior factor under repeated ground motion. They recommended supplementary analyses, particularly for structures with low ductility. Fragiacomo et al. [5] proposed a reduction in the behavior factor after analyzing the response of moment-resistant frames (with rigid and semi-rigid joints) and a braced steel frame subject to repeated ground motion. Luco et al. [6] compared the nonlinear static-pushover approach and nonlinear dynamic analysis to estimate the residual resistance to collapse caused by aftershocks. They showed that the static-pushover approach underestimated the residual capacity. Residual capacity is the difference between original capacity of the structure and the post-earthquake seismic capacity.

Iancovici and Georgiana [7] investigated the effect of repeated ground motions on the behavior and corresponding parameters that are the reasons behind cyclic structural deterioration in response to inelastic response. Maeda and Kang [8] evaluated the residual capacity of low-rise RC structures damaged during earthquakes based on the ratio of residual seismic capacity to initial capacity.

Hatzigeorgiou and Beskos [9] proposed a method to calculate the inelastic displacement ratio of a structure subject to repeated earthquakes. They realized that repeated ground motion has a significant effect on the inelastic displacement ratio. Hatzigeorgiou and Liolios [10] analyzed eight reinforced concrete (RC) frames subjected to 45 sequential ground motions (five real and 40 artificial seismic sequences). They demonstrated that the sequence of the ground motions is important for correct interpretation of the responses.

Moustafa and Takewaki [11] emphasized that multiple ground motions could occur during a short period of time. They found that repeated sequences of earthquakes can result in greater damage to a structure because of the accumulation of inelastic deformation. They presented a stochastic model for repeated acceleration sequences.

Many studies have evaluated seismic structural damage and some researchers have proposed damage indices, which are generally based on three concepts. The first defines the maximum response of a structure as equal to the maximum inter-story drift [12]. The second class is based on cumulative damage [13], where damage to a structure subjected to earthquakes is estimated using static pushover analysis. Chai et al. [14] estimated the plastic strain energy capacity of a structure using the energy-based cumulative damage model. The third class uses a combination of maximum deformation and cumulative damage, such as the damage indices introduced by Park and Ang [15] and Banon and Veneziano [16]. Other studies introducing damage indices can be classified into one of these three classes. For example, the damage index proposed by Zhang et al. [17] for special moment-resisting steel frames includes both maximum deformation and cumulative effects based on a force analogy method (class 3).

Recent studies have evaluated damage indices for structures subjected to mainshock-aftershock sequences. Li and Ellingwood [18] study on the additional damage to steel moment frame due to aftershocks, and they developed a probabilistic approach of structural damage states. Structural response and damage states under mainshock-aftershock sequences are computed using the enhanced uncoupled modal response history analysis method. In their work, simple probabilistic tools are also proposed for rapid structural assessment.

Zhang et al. [19] investigated the effects of aftershocks on the cumulative damage to concrete

gravity dams. Their results reveal that aftershocks have a considerable effect on cumulative damage. Zhai et al. [20] proposed a damage spectrum for mainshock-aftershock earthquakes using the Park-Ang damage index. The damage spectra were calculated using real or simulated mainshock-aftershock records. They also evaluated the effects of spectral period, strength reduction factor, site class, damping ratio, and post-yield stiffness on damage spectra. Joen [21] developed a probabilistic framework to explain vulnerability in terms of damage related to mainshocks.

Polese et al. [22] performed pushover analysis on damaged buildings considering appropriate modification of plastic hinges for damaged elements. Their studies show that in case of minor or moderate damages, the ductility capacity was notably decreased up to 40% (due to the increase of the structure deformability) while the primary structural displacement capacity was not affected considerably. The performance loss is estimated about 15% for minor or moderate damages. The performance loss is reported about 50% for severe damage in their investigation.

Yaghmaei-Sabegh and Ruiz-Garcia [23] studied the nonlinear response of SDOF systems subjected to as-recorded Varzaghan-Ahar seismic sequences that occurred in the North-Western area of Iran on August 11, 2012. The nonlinear response was measured in terms of constant ductility strength reduction factors, *R*, and inelastic displacement ratios, IDR, which were compared with predictive capabilities of previously proposed predictive expressions that take into account seismic sequences. Results indicate that the predictive expressions for R and IDR underestimate values obtained in this study for the intermediate- and long-period spectral region.

Aftershock fragility curves have been proposed to express uncertainty of structural capacity. Zhai et al. [24] investigated the damage to inelastic SDOF structures using different hysteretic models and response-demand parameters. Their results showed that the effect of aftershocks can be disregarded when the ratio of peak ground acceleration (PGA) of aftershocks to mainshock is less than 0.5. Iervolino et al. [25] obtained closed-form estimates for aftershock reliability of elastic perfectly-plastic damage accumulation systems.

Abdelnaby and Elnashai [26] developed a tool that contains appropriate damage features for the numerical analysis of RC structures subjected to more than one earthquake. They also conducted a parametric study that investigates the effects of multiple earthquakes on the response of RC moment resisting frame systems. For this purpose, macroscopic constitutive models of concrete and steel materials that contain the aforementioned damage features and are capable of accurately capturing materials degrading behavior, were selected and implemented into fiber-based finite element software. Furthermore, finite element models that utilize the implemented concrete and steel stress-strain hysteresis were developed. The models are then subjected to selected sets of earthquake sequences. The results indicated that the response of degrading structural systems is appreciably influenced by strong-motion sequences in a manner that cannot be predicted from simple analysis. It also confirms that the effects of multiple earthquakes on earthquake safety can be very considerable.

Zafar and Andrawes [27] studied a new type of reinforcing bars made of fiber reinforced polymer (FRP) with embedded superelastic shape memory alloy (SMA) fibers. SMA-FRP reinforcement is characterized with both ductility and pseudo-elasticity, which are two important characteristics that are sought in this study to enhance the ability of RC moment frames to withstand strong sequential ground motions (i.e. main shock followed by one or more aftershocks). Comparison was drawn between steel and SMA-FRP reinforced frames based on accumulation of damage and residual drifts. Numerical results showed superior performance of SMA-FRP composite reinforced MRF in terms of dissipation of energy and accumulation of lower residual drifts.

Furtadoa et al. [28] studied the mainshock-aftershocks effects on an eight-story RC building. For this, different numerical models (considering different IM walls modelling strategies) were subjected to several non-linear dynamic analyses. The structure damage level was evaluated for different intensity levels of the aftershock-mainshock by the comparison between the maximum inter-story

drifts with drift limits suggested by international codes.

Hosseinpour and Abdelnaby [29] studied effect of different aspects of multiple earthquakes on the nonlinear behavior of RC structures. For this purpose, the nonlinear response of two eight-story reinforced concrete buildings (both regular and irregular in height) was evaluated. The buildings were subjected to a suite of ground motion records obtained from the 2010-2011 Christchurch earthquake sequence. Dynamic response history analyses were conducted to investigate the effects of: 1) damage from previous ground motions; 2) earthquake direction; 3) aftershock polarity; and 4) the vertical component of the earthquake. The results indicated that earthquake direction (in the irregular building), structure irregularity, and the vertical earthquake component could have a considerable effect on the response of structures subjected to multiple earthquakes.

The present investigation first selected 19 mainshock-aftershock earthquake records from the Japan seismic region in which the records for acceleration for the mainshock and its aftershocks were provided by the same station. The characteristics of the mainshock and aftershocks were investigated and compared. Next, a series of RC columns and RC frames having natural periods of 0.1 to 2.5 s were chosen for further analysis. The approaches used to obtain the damage index were: (1) consideration of only mainshock ground motion; (2) consideration of the effect of both mainshock and aftershocks records. The results have led to a proposed modification of the Park-Ang damage index to include aftershock earthquakes. The Park-Ang damage index is chosen in this study as the seismic damage measure, because it is considered as one of the most realistic measures for indicating the structural damage.

2. Ground Motion Records

An important aspect of this study was collocation of a set of ground motion accelerations obtained from mainshock and aftershock earthquakes. A major difficulty in this research was the availability of high-quality ground motion records. In addition, some records lacked data on aftershock earthquake characteristics such as focal depth and magnitude.

K-NET and KiK-net have made available a series of strong ground motions from earthquakes in the Japan seismic region. The organized and reliable operation of these networks has reduced the possibility of missing events in mainshock-aftershock sequences [30]. Furthermore, the availability of high-quality digital data allowed the assured use of the mainshock-aftershock records. Aftershock events occurring within 30 days of the mainshock were selected for use. Within this period of time was considered that rescue operations, recovery activities and repair of structural damages have not been completed; therefore, aftershocks could cause additional damage to mainshock-damaged structures.

Aftershock records with PGA values of less than 0.05 g were excluded from the database unless the number of records for aftershocks was deemed insufficient. The magnitude, focal depth, PGA, significant duration and average S-wave velocity from the database are shown in Table (1). Most of the aftershocks have the moment magnitude more than 4.

Note that the foreshock events were selected in four event sequences (2, 9, 12 and 17) because of the short time interval with the mainshock. In this study, the unprocessed acceleration time series were corrected by both baseline correction and band-pass filtering.

To take into account the effect of free vibration on a structure after the mainshock, the time interval between the sequent events was set at 100 s, as proposed by Hatzigeorgiou and Liolios [9]. For example, a sequent event (event 18) consisting of a mainshock and two aftershocks is shown in Figure (1a). The response spectral acceleration for the three events is shown separately in Figure (1b) and for which the difference in predominant periods is observable.

The values for PGA, predominant frequency (f_p; related to the Fourier amplitude), significant duration (t5-75 and t5-95) for the mainshock and the largest aftershock in the database are shown and compared in Figure (2). The fitted lines and first quarter bisectors are also shown. It is possible to compare the parameters for the mainshock with those for the largest aftershock using the bisector. It can be observed from the figure that, except for f_p, these values are generally larger for the mainshock than for the largest aftershocks.

Table 1. Database selected for mainshock-aftershock sequence.

No.	Sequence	Station	Date	Time	M	Depth (km)	PGA (g)	Significant Duration (s)	Vs (m/s)
1	M	MYG005	Aug. 11, 1996	03:12	5.9	7	0.442	27.35	370
	A1		Aug. 11, 1996	03:54	5.4	10	0.304	16.21	370
	A2		Aug. 11, 1996	05:26	4.3	10	0.096	7.79	370
	A3		Aug. 11, 1996	20:48	4.8	0	0.258	5.63	370
	A4		Aug. 11, 1996	20:52	4.6	10	0.186	5.06	370
	A5		Aug. 13, 1996	11:13	5	10	0.622	3.98	370
	A6		Aug. 14, 1996	07:52	4.2	10	0.172	6.85	370
2	F1	SZO002	Mar. 3, 1997	14:20	4	5	0.124	1.34	315
	F2		Mar. 3, 1997	20:11	4.5	8	0.161	2.19	315
	F3		Mar. 3, 1997	23:09	5	3	0.522	3.05	315
	F4		Mar. 4, 1997	00:03	4.9	0	0.345	1.79	315
	M		Mar. 4, 1997	12:51	5.7	2	0.158	4.92	315
	A1		Mar. 5, 1997	22:43	4.4	2	0.296	1.09	315
	A2		Mar. 7, 1997	02:36	4	8	0.210	1.75	315
	A3		Mar. 7, 1997	16:33	4.6	2	0.294	3.84	315
3	M	KGS005	Mar. 26, 1997	17:31	6.3	8	0.492	5.16	430
	A1		Mar. 26, 1997	17:39	4.7	8	0.158	5.30	430
	A2		Mar. 26, 1997	18:05	4.5	10	0.192	3.97	430
	A3		Mar. 26, 1997	18:30	4	14	0.215	1.62	430
	A4		Mar. 26, 1997	19:45	3.7	10	0.120	1.64	430
	A5		Mar. 26, 1997	22:24	4.4	11	0.150	2.82	430
	A6		Mar. 27, 1997	05:19	3.9	12	0.177	1.31	430
4	M	KGS005	May 13, 1997	14:38	6.2	8	0.872	3.85	430
	A1		May 14, 1997	08:32	4.7	7	0.164	4.51	430
	A2		May 18, 1997	17:49	3.3	10	0.110	0.93	430
	A3		May 25, 1997	06:11	4.4	10	0.239	1.48	430
5	M	HKD133	Mar. 29, 2000	17:22	4.1	7	0.126	3.59	460
	A1		Mar. 29, 2000	20:01	3.6	7	0.149	2.56	460
	A2		Mar. 29, 2000	21:23	3.5	6	0.128	3.05	460
	A3		Mar. 30, 2000	01:26	3.5	7	0.143	2.51	460
	A4		Mar. 30, 2000	02:54	4	7	0.154	3.19	460
6	M	TKY010	Aug. 3, 2000	22:18	6.2	12	0.126	6.73	260
	A1		Aug. 18, 2000	22:51	3.4	2	0.189	65.98	260
	A2		Aug. 19, 2000	12:44	3	3	0.113	4.42	260
	A3		Aug. 29, 2000	11:00	4.9	9	0.282	5.38	260
	A4		Aug. 29, 2000	11:13	3.6	7	0.327	2.49	260
	A5		Aug. 29, 2000	12:08	4.3	6	0.260	5.36	260
7	M	TTR008	Oct. 6, 2000	13:30	7.3	11	0.442	18.03	170
	A1		Oct. 7, 2000	12:03	4.2	9	0.101	3.67	170
	A2		Oct. 8, 2000	20:51	5	9	0.106	7.55	170
	A3		Oct. 10, 2000	21:58	4.4	11	0.103	6.68	170
8	M	MYG011	May 26, 2003	18:24	7	71	1.201	20.57	2000
	A1		May 26, 2003	22:34	4.8	76	0.119	7.89	2000
	A2		May 27, 2003	00:44	4.9	69	0.229	5.36	2000
	A3		May 31, 2003	18:42	4.7	74	0.109	11.44	2000
	A4		June 10, 2003	16:24	4.9	67	0.126	12.55	2000
9	F1	MYG010	July 26, 2003	00:13	5.5	12	0.149	15.25	300
	M		July 26, 2003	07:13	6.2	12	0.210	17.25	300
	A1		July 28, 2003	04:08	5	14	0.147	11.71	300
10	M	HKD100	Sept. 26, 2003	04:50	8	42	1.000	40.27	331
	A1		Sept. 26, 2003	06:08	7.1	21	0.450	33.77	331
	A2		Sept. 29, 2003	11:37	6.5	43	0.102	12.61	331

Table 1. Countine.

No.	Sequence	Station	Date	Time	M	Depth (km)	PGA (g)	Significant Duration (s)	Vs (m/s)
	M		**Oct. 23, 2004**	**17:56**	**6.8**	**13**	**0.599**	**69.01**	**560**
	A1		Oct. 23, 2004	18:03	6.3	9	0.280	6.77	560
	A2		Oct. 23, 2004	18:07	5.7	15	0.131	152.70	560
	A3		Oct. 23, 2004	18:12	6	12	0.269	13.15	560
11	A4	**NIG020**	Oct. 23, 2004	08:09	6.5	14	0.572	122.37	560
	A5		Oct. 23, 2004	19:46	5.7	12	0.156	209.57	560
	A6		Oct. 23, 2004	23:34	5.3	20	0.255	3.06	560
	A7		Oct. 25, 2004	06:05	5.8	15	0.440	8.48	560
	A8		Oct. 27, 2004	10:40	6.1	12	0.534	20.81	560
	F1		Nov. 27, 2004	07:42	5.6	51	0.140	10.87	331
12	M	HKD100	Nov. 29, 2004	03:32	7.1	48	0.140	14.25	331
	A1		Dec. 6, 2004	23:15	6.9	46	0.100	14.03	331
	M		Apr. 21, 2006	02:50	5.8	7	0.376	4.39	315
13	A1	SZO002	Apr. 21, 2006	03:20	4.5	8	0.153	1.68	315
	A2		Apr. 21, 2006	23:17	4.5	9	0.154	1.60	315
	A3		May 2, 2006	18:24	5.1	15	0.229	1.61	315
	M		Mar. 25, 2007	09:42	6.9	11	0.512	10.35	790
14	A1	ISK003	Mar. 25, 2007	18:11	5.3	13	0.268	3.16	790
	A2		Mar. 28, 2007	08:08	4.9	13	0.129	2.84	790
	M		July 16, 2007	10:13	6.8	17	0.633	7.08	190
15	A1	NIG018	July 16, 2007	15:37	5.8	23	0.202	7.78	190
	A2		July 16, 2007	18:19	4.4	22	0.115	2.75	190
	M		June 14, 2008	08:43	7.2	8	0.501	39.21	370
	A1		June 14, 2008	08:52	4	12	0.180	242.00	370
	A2		June 14, 2008	08:58	3.8	5	0.261	2.51	370
	A3		June 14, 2008	08:59	3.6	10	0.103	109.29	370
16	A4	MYG005	June 14, 2008	09:14	3.5	4	0.133	74.89	370
	A5		June 14, 2008	09:20	5.7	6	0.273	21.82	370
	A6		June 14, 2008	11:33	3.4	6	0.139	3.92	370
	A7		June 15, 2008	15:00	3.1	4	0.235	3.94	370
	F1		Dec. 17, 2009	23:45	5	4	0.475	1.84	315
	F2		Dec. 18, 2009	00:40	3.5	6	0.132	2.08	315
	F3		Dec. 18, 2009	02:30	4.2	4	0.125	1.84	315
	F4		Dec. 18, 2009	05:25	4	5	0.144	3.11	315
	M		Dec. 18, 2009	08:45	5.1	5	0.737	1.55	315
	A1		Dec. 18, 2009	16:39	3.9	4	0.105	2.42	315
	A2		Dec. 18, 2009	21:27	3.9	4	0.162	1.44	315
17	A3	SZO002	Dec. 19, 2009	00:53	4.5	4	0.346	1.88	315
	A4		Dec. 19, 2009	01:52	3.7	4	0.112	2.16	315
	A5		Dec. 19, 2009	03:36	3.6	3	0.142	1.86	315
	A6		Dec. 19, 2009	07:58	3.3	4	0.125	1.61	315
	A7		Dec. 19, 2009	18:11	3.9	4	0.173	2.34	315
	A8		Dec. 19, 2009	22:04	4.3	4	0.205	1.87	315
	A9		Dec. 19, 2009	22:09	4.5	4	0.176	1.48	315
	M		Sept. 29, 2010	17:00	5.7	8	0.210	43.89	670
18	A1	FKS025	Sept. 30, 2010	20:05	3.6	8	0.150	0.84	670
	A2		Oct. 1, 2010	08:24	4.4	3	0.079	1.39	670
	M		Mar. 11, 2011	14:46	9	24	3.120	80.86	550
	A1		Mar. 11, 2011	15:09	7.4	32	0.112	218.37	550
	A2		Mar. 11, 2011	15:26	7.5	34	0.096	46.65	550
	A3		Mar. 11, 2011	16:29	6.5	36	0.240	24.18	550
	A4		Mar. 11, 2011	20:37	6.7	24	0.109	160.90	550
19	A5	MYG004	Mar. 24, 2011	17:21	6.2	34	0.176	12.20	550
	A6		Mar. 28, 2011	07:24	6.5	31	0.122	22.93	550
	A7		Apr. 2, 2011	13:08	5.2	42	0.125	7.38	550
	A8		Apr. 7, 2011	23:32	7.1	66	1.211	15.75	550
	A9		Apr. 9, 2011	18:42	5.4	58	0.187	4.91	550

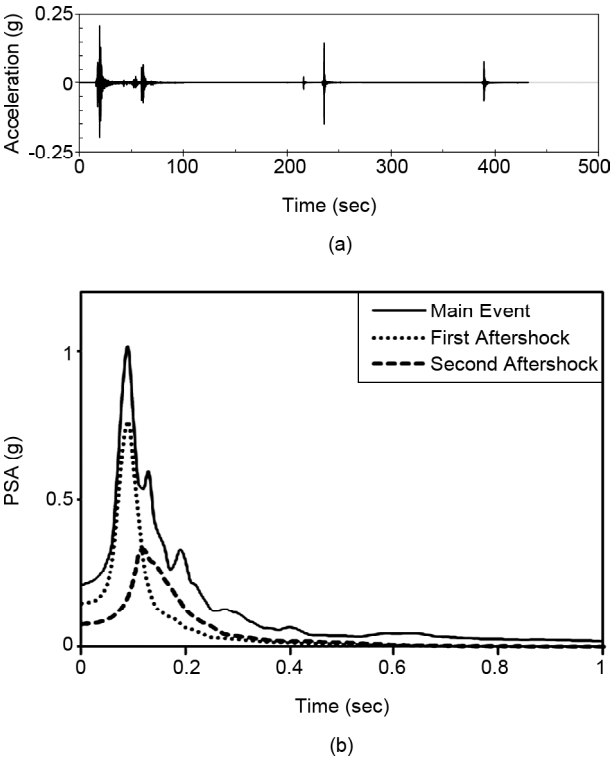

Figure 1. Mainshock and aftershocks for event 18 (Table 1): (a) time series; (b) spectral acceleration.

3. Modeling and Structures

This study used nonlinear dynamic analysis based on the Newmark approach to consider a more realistic behavior for the structures. In the Newmark approach, displacement and velocity at each time step is computed as:

$$u_{i+1} = u_i + (\Delta t)\dot{u}_i + \left((0.5-\beta)(\Delta t)^2\right)\ddot{u}_i + \beta(\Delta t)^2\ddot{u}_{i+1} \quad (1)$$

$$\dot{u}_{i+1} = \dot{u}_i + \left((1-\gamma)\Delta t\right)\ddot{u}_i + \gamma\Delta t\ddot{u}_{i+1} \quad (2)$$

where u_i, $\dot{u}_i$ and $\ddot{u}_i$ are the displacement, velocity and acceleration at time t_i. γ and β show "how much of the acceleration at the end of the interval (Δt) enters into relations for velocity and displacement at the end of the interval" [31]. For more details, it can be referred to Newmark [31].

One important item in nonlinear dynamic analysis is choosing the hysteresis model. In this study, the tri-linear hysteresis model proposed by Park et al. [32] was used. This model considers stiffness degradation, strength deterioration and pinching behavior. These values were set to 2, 0.1 and infinity, respectively, based on the modified Takeda model. Nonlinear analysis was done using IDARC 2D

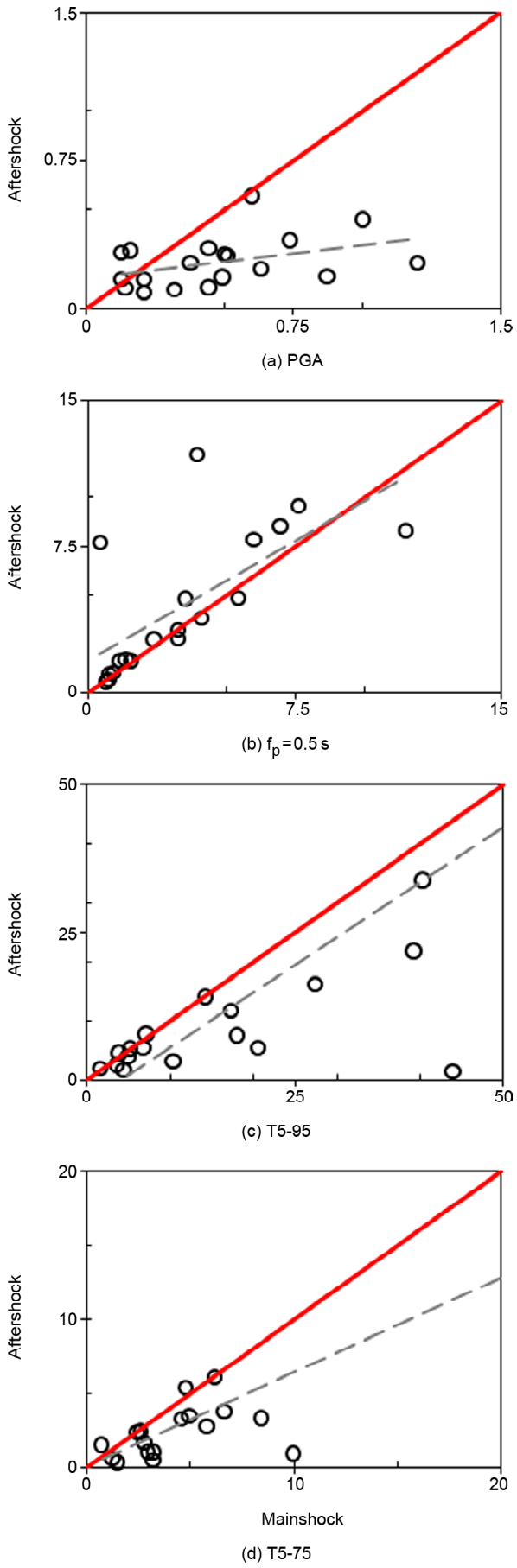

Figure 2. Comparison of ground motion characteristics of mainshock with largest aftershock, (a) PGA, (b) f_p, (c) t5-95, (d) t5-75.

version 5.5 [33] to estimate the damage index. The damage index introduced by Park and Ang is as follows:

$$DI_{PA} = \frac{\delta_m}{\delta_u} + \frac{\beta}{Q_u \delta_u} \int dE \quad (3)$$

where δ_m is the maximum deformation in response to an earthquake, δ_u is the ultimate deformation under monotonic loading of the elements, Q_u is yield strength, dE is incremental absorbed hysteric energy, and β is the effect of cyclic loading on structural damage which is set to 0.1.

Since the mid-1980s, the effectiveness of using the Park-Ang and other similar damage indices has been studied by many researchers [34]. A comparison of various damage indices has been performed in many researches [35-38] that show the effectiveness of Park-Ang damage index. The Park-Ang damage index is found to be in more agreement with laboratory results by assessing the damage potential from various indices and comparing them with experimental observations in the study of Kunnath and Jenne [38]. A comprehensive study on the comparison of different structural damage indices have been carried out by Williams and Sexsmith [39]. With its appropriateness in indicting the actual damage of the structures (RC, Steel, timber) [32, 40], and also its applicability to different hysteresis characteristics, the Park-Ang damage index is preferred for structural damage index in this study. Overall damage can be stated as [15]:

$$DI_T = \sum \left[(\lambda_i)_{story} \times (DI_i)_{story} \right] \quad (4)$$

$$\lambda_i = \left(\frac{E_i}{\sum E_i} \right)_{story} \quad (5)$$

where DI_i is the damage index of each story and λ_i is the weighting coefficient corresponding to the energy contribution factor. These are calculated using the following relations:

$$DI_{story} = \sum \left[(\lambda_i)_{member} \times (DI_i)_{member} \right] \quad (6)$$

$$\lambda_{member} = \left(\frac{E_i}{\sum E_i} \right)_{member} \quad (7)$$

The degree of damage, the damage index and physical appearance for structures are shown and defined in Table (2).

The mainshock accelerations were normalized to the level at which the structures experienced nonlinear behavior and the degree of damage was obtained for at least the moderate level (discussed in the following section). This allowed investigation of the effect of the aftershocks.

Two types of structures were considered for further analysis. First, a series of columns with lumped mass were studied at different periods of vibration; a column with lumped mass can be considered as a simplified model of a bridge pier and its deck. For this case, records for 13 circular columns with different section details and masses at 13 periods of vibration from 0.1 to 3 s were selected for further analysis. Table (3) provides details of the chosen sections.

Next, a one-story, three-bay RC frame was analyzed and designed using the response spectrum method considering UBC 2006 provisions. In this study, the column height varied from 3 m to 6 m and span is equivalent to 5 m. The dead and live loads were assumed to be 625 and 200 kg/m^2, respectively. The ultimate tensile strength of the steel was assumed to be 400 MPa and of the compressive strength of the concrete to be 25 MPa. The modulus of elasticity for the steel and concrete was 200 and 25 GPa, respectively. Details of the sections selected for the beam and column elements are shown in Table (4).

Damage analysis was performed on one bay of the frame at different predominant periods to

Table 2. Damage inspection [24].

Degree of Damage	Physical Appearance	Damage Index	Condition
Collapse	Total or Partial Collapse of Building	1	Threat to Human Lives
Severe	Extensive Crashing of Concrete. Disclosure of Buckled Reinforcements	0.4-1	Loss of Building
Moderate	Extensive Large Cracks. Spalling of Concrete in Weaker Elements	0.25-0.4	Repairable
Minor	Minor Cracks Throughout Building. Partial Crushing of Concrete in Columns	0.1-0.25	Repairable
Slight	Sporadic Occurrence of Cracking	<0.1	Repairable

Table 3. Details of circular column sections.

Period (s)	Diameter of Section (mm)	Column Height (mm)	Lumped Mass (kN)	Longitude Bars	Transverse Bars
0.1	550	2000	100	6Φ10	Φ10 @ 100 mm
0.3	600	3500	300	16Φ20	Φ10 @ 100 mm
0.5	600	4000	600	20Φ24	Φ10 @ 100 mm
0.7	700	4000	1500	24Φ30	Φ10 @ 100 mm
1	800	4500	6000	34Φ30	Φ10 @ 100 mm
1.3	800	5200	7000	40Φ30	Φ10 @ 100 mm
1.5	900	6500	7500	40Φ34	Φ10 @ 100 mm
1.7	900	6800	10000	40Φ40	Φ10 @ 100 mm
2	1500	11000	22500	80Φ40	Φ10 @ 100 mm
2.3	1500	11500	26000	80Φ40	Φ10 @ 100 mm
2.5	1500	12000	28000	80Φ40	Φ10 @ 100 mm
2.7	1800	14000	38000	100Φ40	Φ10 @ 100 mm
3	1800	14500	43000	100Φ40	Φ10 @ 100 mm

Table 4. Section details for one-story, three-bay RC frame.

Elements	Section Type	Dimension (mm)	Longitude Bars	Transverse Bars
Column	Rectangular	350 × 350	12Φ20	Φ10@100 mm
Beam	Rectangular	400 × 300	Top: 3Φ20 Bot: 3Φ20	Φ10@100 mm

investigate the effect of aftershocks on the structure considering both the beam and column elements. Note that the mass and height of the frame was increased to obtain different periods for the frame. The frames were investigated for a set of 25 periods of vibration from 0.1 to 2.5 s with an interval of 0.1 s. Analysis of these structures to obtain a damage index considering the effect of aftershocks is discussed in the following sections.

4. Damage Index Analysis

4.1. Circular RC Column

The damage index (*DI*) for circular columns was calculated for 19 earthquake events. A moderate degree of damage was achieved by scaling the mainshock records using scaling factors of greater or less than 1. The aftershock records are also multiplied by this scaling factor.

After the structures had sustained moderate damage from the mainshock, the aftershocks were applied. The *DI* values derived for the mainshock and by the mainshock + aftershocks were calculated at four periods (T = 0.1, 0.5, 1, 2 s) for all events. The results are shown in Figure (3), where the horizontal axis provides the event number shown in Table (1).

Figure (3) shows that the calculated *DI* changed at each period in response to the mainshock event and the aftershock incidents. These changes are more noticeable for the long periods; therefore, it can be understood that structures damaged during distant events are more at risk from the effects of aftershocks. The greatest change was recorded for periods of 1 to 3 s.

The average *DI* for all events for each period is shown in Figure (4). The figure indicates dispersion in the variation in *DI* (ΔDI) for each period when considering the only mainshock and then including the aftershocks. It can be said that the differences in *DI* for long periods (more than 1 s) are more evident.

The most damage was recorded for sequent events in which the PGA of the aftershocks was larger than the PGA of the mainshock. These were events 1, 2, 5, 6, 11, 12, 13 and 17 from Table (1). The relation between ΔDI and the period of the vibration can be obtained by regression analysis of the results of Figure (4) as:

$$\Delta DI = 0.081T + 0.0466,\ R^2 = 0.7379 \quad (8)$$

It can be said that structures characterized by longer periods experience more damage during aftershocks. For periods of <0.5 s, the increase in *DI* from an aftershock is close to 0.1, although for longer periods (> 0.5 s) this value can reach 0.4. The ratio of ΔDI from aftershocks to the *DI* from the mainshock was calculated for each period

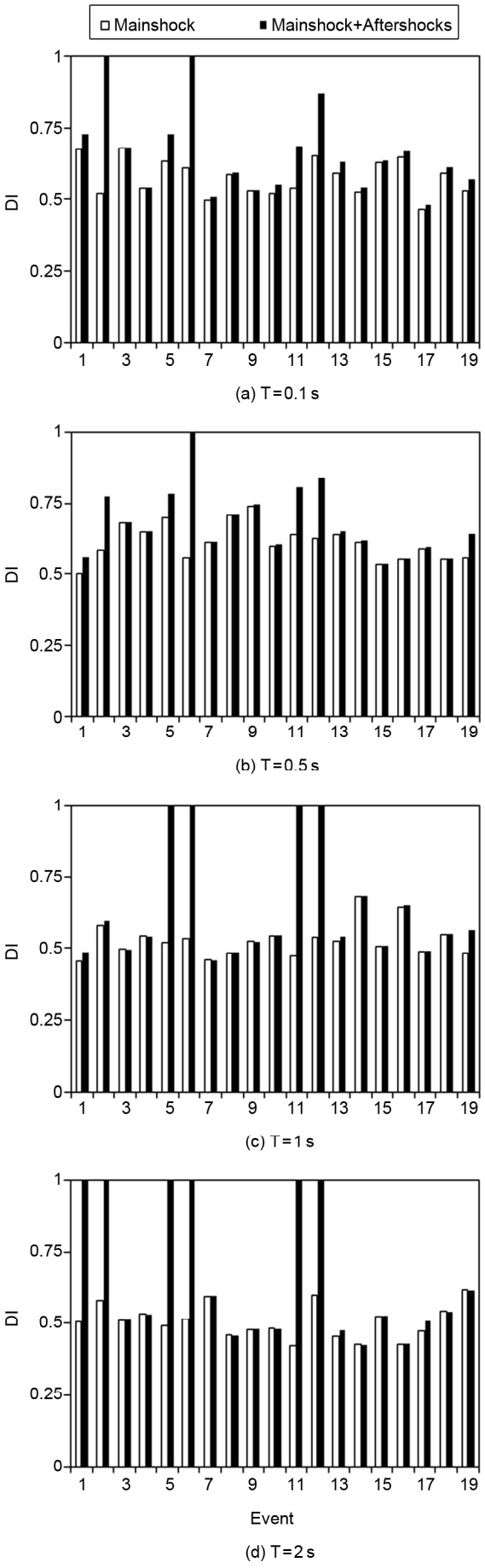

Figure 3. Variation in DI of circular columns versus event, (a) T = 0.1 s, (b) T = 0.5 s, (c) T = 1 s, (d) T = 2 s.

(Figure 5). This ratio generally correlated with the period of the structure; in other words, the ratio increased as softening of the structure increased.

Figure (6) shows the ΔDI versus time for the circular column with period of 2 s in response to event 1 (Table 1). The destructive effect of the

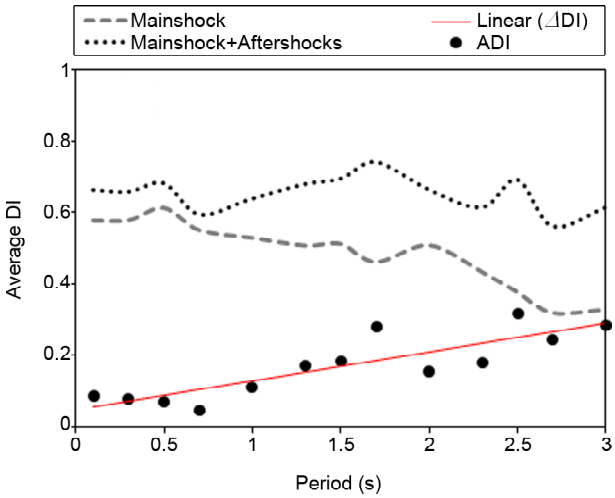

Figure 4. Average DI for circular columns versus period.

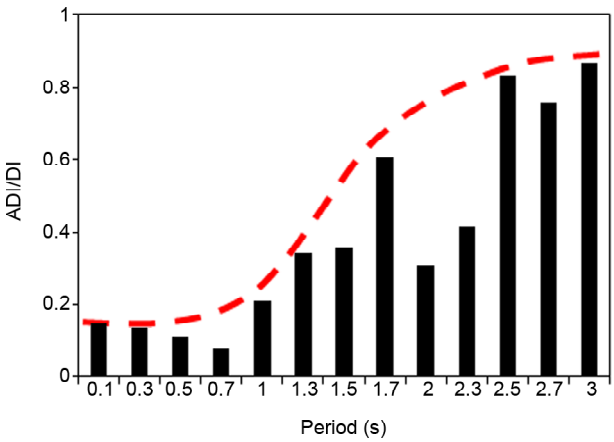

Figure 5. Ratio of ΔDI to DI from mainshock.

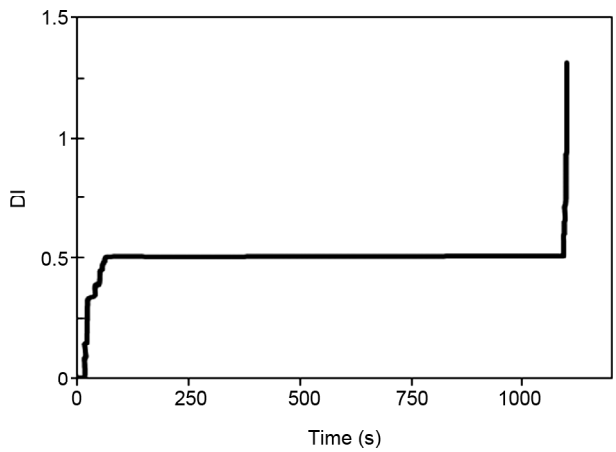

Figure 6. Time history of DI for circular columns subjected to event 1 at 2 s periods.

aftershocks is evident. The *DI* for the mainshock was ~0.51; after the fifth aftershock, it was ~1.40 (considered as 1). This means that this aftershock caused the collapse of the structure and demonstrates the importance of consideration of the destructive effects of the aftershocks. These results can be used to modify the *DI* parameters introduced by Park and Ang by considering the effects of the aftershocks to:

$$DI_{Aftershocks} = DI_{PA} + \Delta DI \tag{9}$$

4.2. One-Story, One-Bay RC Frame

The DI for the RC frames was computed for all earthquake events. The results here have been provided for the beam and column elements. Analysis shows that the beams sustained more damage than the columns under seismic loading. In sec. 3.1, the variation in *DI* from sequent events having aftershocks with larger PGA values was more noticeable. The average DI of all events for each period is shown in Figure (7). The DI for columns for four periods versus the event number is shown in Figure (8).

As for circular columns (sec. 3.1), the variation in DI are different for lower and longer periods. This variation is greater for longer periods (0.5 and 2 s). The average ?DI for beam and column elements for each period is shown in Figure (9). Earthquake events 1, 2, 5, 6, 11, 12 and 13 (Table 1) show a greater increase in *DI* in response to the aftershocks. The ratio of the PGA for the largest aftershock to the mainshock for these events was 1.41, 1.87, 1.20, 2.60, 0.96, 0.71 and 0.61, respectively. It is evident that these ratios, which increased damage, are greater

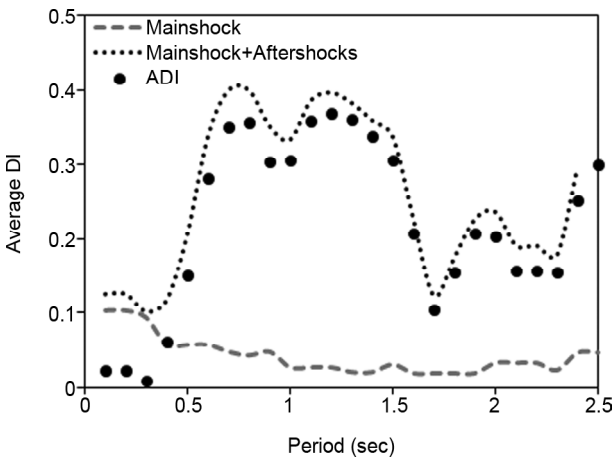

Figure 7. Average DI for column element versus period.

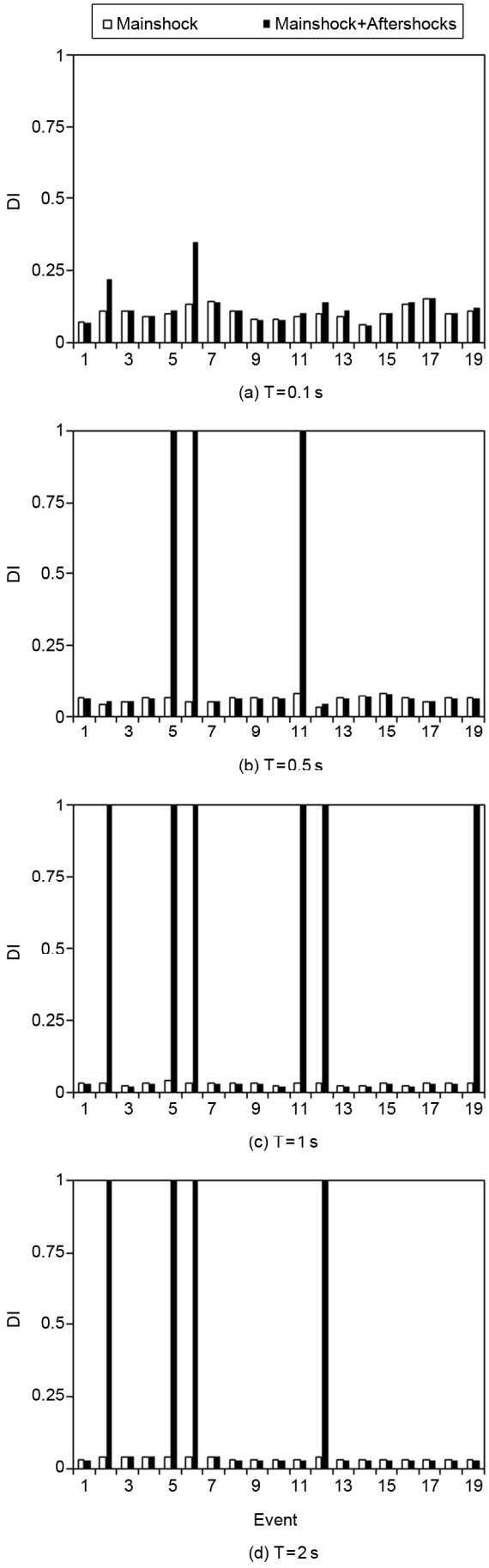

Figure 8. Calculated DI for column elements versus event, (a) T = 0.1 s, (b) T = 0.5 s, (c) T = 1 s, (d) T = 2s.

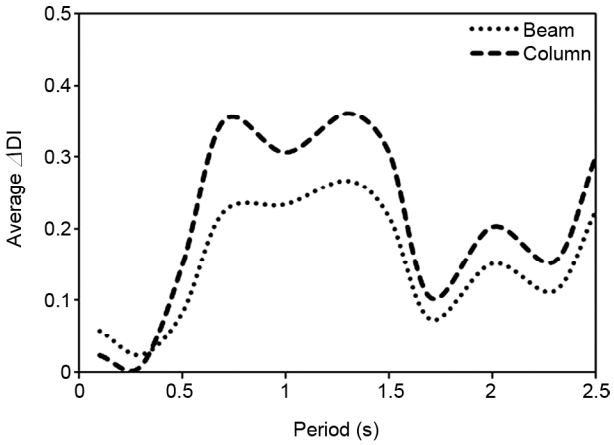

Figure 9. Average variation in DI for beam and column elements versus period.

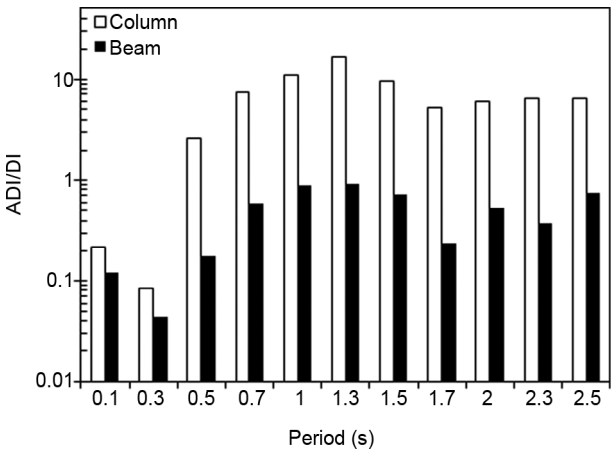

Figure 10. ΔDI/DI from mainshock for beam and column elements versus period.

than 0.6. The ratio of ΔDI to the estimated DI from the mainshock is plotted in Figure (10). It appears that the ratio increased up to a specific period; at longer periods, this ratio appears to be constant.

The average maximum displacement for all frames in response to the mainshock and the mainshock + aftershock is shown in Figure (11). The figure shows that the displacement terms for the aftershocks are remarkable. The DI caused by accumulated energy is illustrated in Figure (11b). It can be seen that the effect of this term is negligible and is less than 0.03.

5. Modified Damage Index

A relation to modify the damage index proposed by Park and Ang [15] was developed based on the results obtained from the analysis of RC frames. The damage index undergoes changes during different periods. It has been observed that aftershocks with larger PGA values than the mainshock result in greater ΔDI values (ratio of PGA for largest aftershock to mainshock; usually > 0.6).

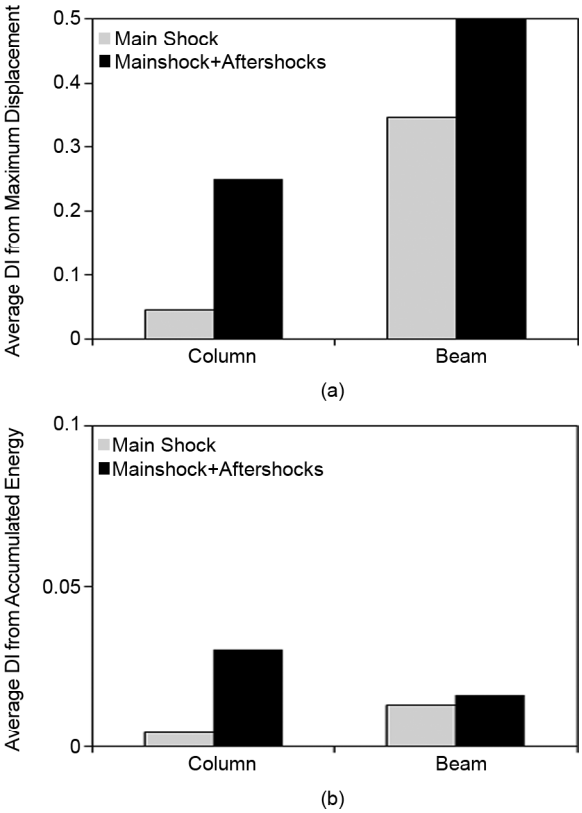

Figure 11. Average DI from (a) maximum displacement and (b) accumulated energy.

The relationship between the period of vibration and the DI was next investigated. Modification terms were added to the DI to consider the effect of aftershocks. It was shown that there is a relationship between the DI and the period showing a curve. This curve was simplified using four lines having different slopes (Figure 12). The figure shows the proposed lines for calculating ΔDI for the beam and column elements versus the predominant period of the structure. The slopes of the lines illustrate the specific behavior of structures subject to aftershocks.

The four lines used to estimate ΔDI can be computed for beams and columns as:

$$\Delta DI_{Aftershocks} = A \times T + B \tag{10}$$

where A and B are the slope and intercept, respectively. These parameters were calculated for the RC frames and the results are shown in Table (5).

Equation (10) can be added to Park-Ang DI as a dimensionless term as follows using the previously-

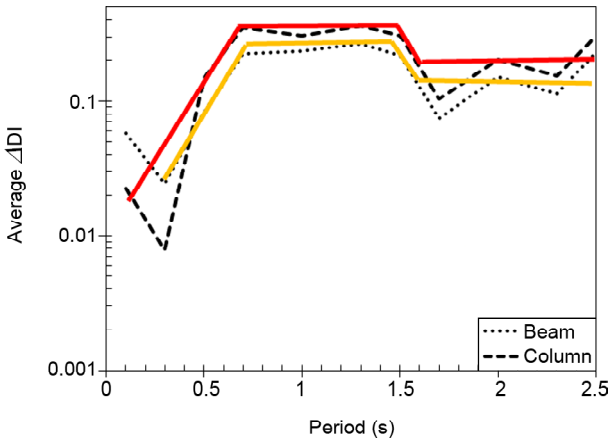

Figure 12. Proposed model for ΔDI of beam (yellow line) and column (red line) elements versus predominant period.

Table 5. Slope and intercept of RC frames.

Element	Period (s)	A	B
Column	$T < 0.7$	0.57	-0.04
	$0.7 \le T < 1.5$	0	0.36
	$1.5 \le T < 1.6$	-1.6	2.76
	$T \ge 1.6$	0	0.2
Beam	$T < 0.7$	0.525	-0.0975
	$0.7 \le T < 1.5$	0	0.27
	$1.5 \le T < 1.6$	-1.2	2.07
	$T \ge 1.6$	0	0.15

defined variables:

$$DI_{PA} = \frac{\delta_m}{\delta_u} + \frac{\beta}{Q_u \delta_u} \int dE + \Delta DI_{Aftershocks} \qquad (11)$$

6. Conclusion

The effect of multiple earthquakes on structures has been ignored in seismic design codes and damage estimation. Most major earthquakes are followed by many aftershocks. Examples of this include the Northridge (1994), Kocaeli (1999), Haiti (2010), Emilia (2012), Gorkha (2015), and Sarpol-e Zahab (2017) earthquakes. Aftershocks can cause severe damage or collapse of a damaged structure from heightened vulnerability. The safety of occupants can be threatened by damage to structures caused by aftershocks. Mainshock-damaged buildings are more prone to cumulative damage caused by aftershocks because "their reduced structural capacity exacerbates the threshold of the ground motion intensity needed to cause further damage" [21].

The behavior of structures subjected to a mainshock and its aftershocks was investigated in this study. It was shown that the characteristics of aftershocks can differ from the mainshock. For example, the PGA of aftershocks could be larger than that of the mainshock. The variation in damage index is more evident when the PGA of the largest aftershock and the mainshock are similar. In other word, it has been observed that aftershocks with larger PGA values than the mainshock (where the ratio of PGA for largest aftershock to mainshock is usually > 0.6) result in greater damage index values.

The average ΔDI was different for different periods, although these differences were more significant for long periods. In short periods, ΔDI increased as the period increased. In the middle periods, the variation can be assumed to be constant with the highest values recorded for the beam and column elements. In long periods, the variation can be considered constant and lower than the proposed ΔDI for middle periods.

The DI for maximum displacement and cumulative hysteretic energy were evaluated for RC frames. The most destructive effects of aftershocks are for maximum displacement, which may induce ultimate displacement the beam and column elements.

A dimensionless term is proposed for addition to the Park-Ang damage index for RC frames that includes the effects of aftershocks. The value of the dimensionless term depends on the period and the type of element (column or beam).

References

1. Ruiz-Garcia, J. (2012) Mainshock-aftershock ground motion features and their influence in building's seismic response. *Journal of Earthquake Engineering*, **16**(5), 719-737.

2. Sunasaka, Y. and Kiremidjian, A.S. (1993) *A Method for Structural Safety Evaluation Under Mainshock-Aftershock Earthquake Sequences*. John A. Blume Earthquake Engineering Center.

3. Gallagher, R.P., Reasenberg, P., and Poland, C.D. (1999) Earthquake aftershocks: entering damaged buildings. Applied Tech Council.

4. Amadio, C., Fragiacomo, M., and Rajgelj, S. (2003) The effects of repeated earthquake ground

motions on the non-linear response of SDOF systems. *Earthquake Engineering and Structural Dynamics*, **32**, 291-308.

5. Fragiacomo, M., Amadio, C., and Macorini, L. (2004) Seismic response of steel frames under repeated earthquake ground motions. *Engineering Structures*, **26**, 2021-2035.

6. Luco, N., Bazzurro, P., and Cornell, C.A. (2004) Dynamic versus static computation of the residual capacity of a mainshock-damaged building to withstand an aftershock. *Presented at 13th World Conference on Earthquake Engineering*, Vancouver, Canada, paper#2405.

7. Iancovici, M. and Georgiana, I. (2007) Evaluation of the inelastic demand of structures subjected to multiple ground motions. *Journal of Structural Engineering*, **4**, 143-154.

8. Maeda, M. and Kang, D.E. (2009) Post-earthquake damage evaluation of reinforced concrete buildings. *Journal of Advanced Concrete Technology*, **7**, 327-335.

9. Hatzigeorgiou, G.D. and Beskos, D.E. (2009) Inelastic displacement ratios for SDOF structures subjected to repeated earthquakes. *Engineering Structures*, **31**, 2744-2755.

10. Hatzigeorgiou, G.D. and Liolios, A.A. (2010) Nonlinear behaviour of RC frames under repeated strong ground motions. S*oil Dynamic and Earthquake Engineering*, **30**, 1010-1025.

11. Moustafa, A. and Takewaki, I. (2011) Response of nonlinear single-degree-of-freedom structures to random acceleration sequences. *Engineering Structures*, **33**, 1251-1258.

12. Powell, G.H. and Allahabadi, R. (1988) Seismic damage prediction by deterministic methods: concepts and procedures. *Earthquake Engineering and Structural Dynamics*, **16**, 719-734.

13. Ghobarah, A., Abou-Elfath, H., and Biddah, A. (1999) Response-based damage assessment of structures. *Earthquake Engineering and Structural Dynamics*, **28**, 79-104.

14. Chai, Y.H., Fajfar, P., and Romstad, K.M. (1998) Formulation of duration-dependent inelastic seismic design spectrum. *Journal of Structural Engineering*, **124**, 913-921.

15. Park, Y.J. and Ang, A.H.S. (1985) Mechanistic seismic damage model for reinforced concrete. *Journal of Structural Engineering*, **111**, 722-739.

16. Banon, H. and Veneziano, D. (1982) Seismic safety of reinforced concrete members and structures. *Earthquake Engineering and Structural Dynamics*, **10**, 179-193.

17. Zhang, X., Wong, K.K., and Wang, Y. (2007) Performance assessment of moment resisting frames during earthquakes based on the force analogy method. *Engineering Structures*, **29**, 2792-2802.

18. Li, Q. and Ellingwood, B.R. (2007) Performance evaluation and damage assessment of steel frame buildings under main shock-aftershock earthquake sequences. *Earthquake Engineering and Structural Dynamics*, **36**(3), 405-427.

19. Zhang, S., Wang, G., and Sa, W. (2013) Damage evaluation of concrete gravity dams under mainshock-aftershock seismic sequences. *Soil Dynamic and Earthquake Engineering*, **50**, 16-27.

20. Zhai, C.H., Wen, W.P., Chen, Z., Li, S., and Xie, L.L. (2013) Damage spectra for the mainshock-aftershock sequence-type ground motions. *Soil Dynamic and Earthquake Engineering*, **45**, 1-12.

21. Jeon, J.S. (2013) *Aftershock Vulnerability Assessment of Damaged Reinforced Concrete Buildings in Californi*a. Ph.D. Thesis, Georgia Institute of Technology, USA.

22. Polese, M., Di-Ludovico, M., Prota, A., and Manfredi, G. (2013) Damage-dependent vulnerability curves for existing buildings. *Earthquake Engineering and Structural Dynamics*, **42**(6), 853-870.

23. Yaghmaei-Sabegh, S. and Ruiz-Garcia, J. (2016) Nonlinear response analysis of SDOF systems subjected to doublet earthquake ground motions: A case study on 2012 Varzaghan-Ahar events. *Engineering Structures*, **110**, 281-292, DOI:

10.1016/j.engstruct.2015.11.044.

24. Zhai, C.H., Wen, W.P., Li, S., Chen, Z., Chang, Z., and Xie, L.L. (2014) The damage investigation of inelastic SDOF structure under the mainshock-aftershock sequence-type ground motions. *Soil Dynamic and Earthquake Engineering*, **59**, 30-41.

25. Iervolino, I., Giorgio, M., and Chioccarelli, E. (2014) Closed?form aftershock reliability of damage-cumulating elastic perfectly-plastic systems. *Earthquake Engineering and Structural Dynamics*, **43**, 613-625.

26. Abdelnaby, A.E. and Elnashai, A.S. (2015) Numerical modeling and analysis of RC frames subjected to multiple earthquakes. *Earthquakes and Structures*, **9**(5), 957-981, DOI: 10.12989/eas.2015.9.5.957.

27. Zafar, A. and Andrawes, B. (2015) Seismic behavior of SMA-FRP reinforced concrete frames under sequential seismic hazard. *Engineering Structures*, **98**, 163-173, DOI: 10.1016/j.engstruct.2015.03.045.

28. Furtado, A., Rodrigues, H., Arêde, A., and Varum, H. (2017) Assessment of the mainshock-aftershock collapse vulnerability of RC structures considering the infills in-plane and out-of-plane behavior. *Procedia Engineering*, **199**, 619-624, https://doi.org/10.1016/j.proeng.2017.09.107.

29. Hosseinpour, F. and Abdelnaby, A.E. (2017) Effect of different aspects of multiple earthquakes on the nonlinear behavior of RC structures. *Soil Dynamics and Earthquake Engineering*, **92**, 706-725. DOI: 10.1016/j.soildyn.2016.11.006.

30. www.kyoshin.bosai.go.jp.

31. Newmark, N.M. (1959) A method of computation for structural dynamics. *Journal of Engineering Mechanics Division*, **85**, 67-94.

32. Park, Y.J., Ang, A.H., and Wen, Y.K. (1987) Damage-limiting aseismic design of buildings. *Earthquake Spectra*, **3**, 1-26.

33. Valles, R.E., Reinhorn, A.M., Kunnath, S.K., Li, C., and Madan, A. (1996) *IDARC-2D Version 5.5: A Program for the Inelastic Damage Analysis of Buildings*.

34. Ghosh, S., Datta, D., and Katakdhond, A.A. (2011) Estimation of the Park-Ang damage index for planar multi-storey frames using equivalent single-degree systems. *Engineering Structures*, **33**(9), 2509-2524.

35. Fajfar, P. (1992) Equivalent ductility factors, taking into account low-cycle fatigue. *Earthquake Engineering and Structural Dynamics*, **21**(10), 837-48.

36. Carr, A.J. and Tabuchi, M. (1993) The structural ductility and the damage index for reinforced concrete structure under seismic excitation. *2nd European Conference on Structural Dynamics*, **1**, 169-76.

37. Cosenza, E., Manfredi, G., and Ramasco, R. (1993) The use of damage functionals in earthquake engineering: a comparison between different models. *Earthquake Engineering and Structural Dynamics*, **22**(10), 855-68.

38. Kunnath, S.K. and Jenne, C. (1994) Seismic damage assessment of inelastic RC structures. In: *5th US National Conference on Earthquake Engineering*, **1**, 55-64.

39. Williams, M.S. and Sexsmith, R.G. (1995) Seismic damage indices for concrete structures: a state-of-the-art review. *Earthquake Spectra*, **11**(2), 319-49.

40. Van de Lindt, J.W. (2005) Damage-based seismic reliability concept for woodframe structures. *Journal of Structural Engineering, ASCE*, **131**(4), 668-75.